

Particle Based Visualization of Stress Distribution Caused by the Aortic Valve Deformation

Masashi Nakagawa¹, Nobuhiko Mukai²,
Kiyomi Niki³, and Shuichiro Takanashi⁴, Non-members

ABSTRACT

Medical and engineering technologies have developed the surgical simulators, which allow users to train for surgical skills. To perform the aortic valve replacement, which is one of the cardiovascular surgeries, it is necessary to examine not only the timing of the heart pulsating but also the stress distribution on the aortic valve. For pre-operative planning, we have visualized the stress on the aortic valve due to the deformation of the aorta and blood stream. In our research, simulations of the deformation of the aortic valve and blood stream have been performed with 3D aorta and aortic valve models, which are composed of particles. In the simulation, the aortic valve and blood models are treated as an elastic body and Hershel-Bulkley fluid, respectively. We have used MPS (Moving Particle Semi-implicit) as the particle method; however, it is known that MPS method cannot specify the stress because the pressure among the particles on the free surfaces is zero. Then, in this paper, we propose more stable pressure calculation by considering virtual particles. As a result, visualization of the stress distribution on the aortic valve has been achieved.

Keywords: Visualization, Particle Method, Aortic Valve, Stress Distribution

1. INTRODUCTION

Recently, in the field of the cardiovascular surgery, the aortic valve replacement or the aortic valve plasty, which are the surgeries of the aortic valve shape, is performed to the patients who have the valvular disease [1]. In these surgeries, the heart pulse and the valve's opening and closing timing have to be examined during the operations. In addition, the stress distribution during the surgeries should be visualized.

In these simulations, two kinds of models are used: MSM (Mass Spring Model) that constructs organs

with masses and springs, and FEM (Finite Element Model) that constructs organs with tetrahedral elements. These models, however, are needed to be reconstructed for topological change of models such as bleeding. Then, for these simulations, particle method [2] is used as a new method that can be applied for topological change. There are two kinds of particle methods: SPH (Smoothed Particle Hydrodynamics) and MPS (Moving Particle Semi-implicit). SPH method considers that the velocity and the density of a particle are smoothly distributed around the particle, while MPS method considers that they are placed at the center of a particle. For the simulation of incompressible fluid, MPS method can be used; however SPH method cannot be applied so that ISPH (Incompressible SPH) [3] method, which is another method developed for incompressible fluid, is used. Example researches with particle methods include deformation analysis of red cells flowing in blood vessels [4], and bleeding simulation caused by cutting a blood vessel [5]. In our research, blood stream inside of the aorta, and opening and closing of the aortic valve are simulated, and the stress distribution on the aortic valve is visualized.

2. GOVERNING EQUATIONS

Governing equations of continuum body such as the aortic valve and blood are Cauchy's equation of motion, equation of continuity and constitutive equation of materials. The detailed explanation is the following.

2.1 Governing Equation of Continuum

Cauchy's equation of motion that expresses conservation of momentum, and equation of continuity that expresses conservation of mass, are formulated as Eqs.(1) and (2).

$$\rho \frac{D\mathbf{v}}{Dt} = \nabla \cdot \boldsymbol{\sigma} + \mathbf{F} \quad (1)$$

$$\frac{D\rho}{Dt} + \rho \nabla \cdot \mathbf{v} = 0 \quad (2)$$

Where, ρ is density, v is velocity, t is time, $\boldsymbol{\sigma}$ is stress tensor and \mathbf{F} is external force.

Manuscript received on March 15, 2011 ; revised on April 15, 2012.

^{1,2,3} The authors are with Graduate School of Engineering, Tokyo City University, Japan. , E-mail: nakagawa@vgl.cs.tcu.ac.jp, mukai@cs.tcu.ac.jp and niki@bme.tcu.ac.jp

⁴ The author is with Dept. of Cardiovascular Surgery, Sakakibara Heart Institute, Japan. , E-mail: takanashi-s@gem.hiho.ne.jp

2.2 Constitutive Equation of the Aortic Valve

Constitutive equation of an elastic body is written as Eq.(3), and is applied to the aortic valve.

$$\boldsymbol{\sigma}^e = \lambda \text{tr}(\boldsymbol{\varepsilon})\mathbf{I} + 2G\boldsymbol{\varepsilon} \quad (3)$$

$$\boldsymbol{\varepsilon} = \frac{1}{2} (\nabla \mathbf{u} + (\nabla \mathbf{u})^T) \quad (4)$$

Where, $\boldsymbol{\sigma}^e$ is stress of elastic body, $\boldsymbol{\varepsilon}$ is strain tensor, \mathbf{I} is unit tensor, \mathbf{u} is displacement, λ and G are lame constants that are expressed as the following.

$$\lambda = \frac{vE}{(1+v)(1-2v)} \quad (5)$$

$$G = \frac{E}{2(1+v)}$$

Where, E is Young's modulus and v is Poisson's ratio. By substituting Eqs.(3) and (4) into Cauchy's equation of motion (Eq.(1)), Cauchy-Navier equation (Eq.(6)) can be obtained as follows.

$$\rho \frac{D^2 \mathbf{u}}{Dt^2} = (\lambda + G)\nabla(\nabla \cdot \mathbf{u}) + G\nabla^2 \mathbf{u} + \mathbf{F} \quad (6)$$

2.3 Constitutive Equation of Blood

Since blood is non-Newtonian fluid that yields stress, it can be approximated by Herschel-Bulkley fluid or Casson fluid. Herschel-Bulkley fluid is more similar to the characteristic of blood than Casson fluid [6]. The constitutive equation of Herschel-Bulkley fluid is given as follows.

$$\boldsymbol{\sigma}^f = -p\mathbf{I} + 2\mu\mathbf{D} \quad (7)$$

$$\mu = mD^{n-1} + \frac{\tau_0}{D} \quad (8)$$

$$D = \sqrt{2\mathbf{D} : \mathbf{D}} \quad (9)$$

$$\mathbf{D} = \frac{1}{2} (\nabla \mathbf{v} + (\nabla \mathbf{v})^T) \quad (10)$$

Where, $\boldsymbol{\sigma}^f$ is stress of fluid, p is pressure, μ is viscosity, \mathbf{D} is rate of strain tensor, m and n are constants depending on hematocrit, τ_0 is yield stress, and v is velocity. Navier-Stokes equation (Eq.(11)) is obtained by substituting Eqs.(7) and (10) into Cauchy's equation of motion (Eq.(1)).

$$\rho \frac{D\mathbf{v}}{Dt} = -\nabla p + \mu \nabla^2 \mathbf{v} + \mathbf{F} \quad (11)$$

Since Herschel-Bulkley fluid yields stress, viscosity μ in Eq.(8) is used if the condition of Eq.(12) is satisfied. Otherwise, tensor \mathbf{D} is considered as zero by making viscosity μ huge so that $\boldsymbol{\tau}$ should be zero.

$$\frac{1}{2} \boldsymbol{\tau} : \boldsymbol{\tau} = \tau_0^2 \quad (12)$$

$$\boldsymbol{\tau} = 2\mu\mathbf{D} \quad (13)$$

3. MPS METHOD

It is necessary to discretize partial differential equations used in the governing equations and MPS method uses weight function for it, which function is defined based on the distance between particles. The weight function is given as follows.

$$w(|\mathbf{r}_{ij}|) = \begin{cases} \frac{r_e}{|\mathbf{r}_{ij}|} & (0 \leq |\mathbf{r}_{ij}| < r_e) \\ 0 & (|\mathbf{r}_{ij}| \geq r_e) \end{cases} \quad (14)$$

Where, \mathbf{r} is position vector of a particle, \mathbf{r}_{ij} is the difference between position vectors of particle i and j , and r_e is called radius of effect, and particles within the radius affect the center particle. The weight function uses the current distance between particles in the fluid model. On the other hand, it uses the initial distance between particles in the elastic model. The summation of the weight function for all particles within the radius of effect becomes particle density as follows.

$$n_i \sum_{j \neq i} w(|\mathbf{r}_{ij}|) \quad (15)$$

Where, the particle density in uncompressed state is n^0 . Here, gradient, divergence, and Laplacian models in MPS are defined as the following.

$$\langle \nabla \phi \rangle_i = \frac{d}{n^0} \sum_{j \neq i} \frac{\phi_j - \phi_i}{|\mathbf{r}_{ij}|^2} \mathbf{r}_{ij} w(|\mathbf{r}_{ij}|) \quad (16)$$

$$\langle \nabla \cdot \nabla \phi \rangle_i = \frac{d}{n^0} \sum_{j \neq i} \frac{(\phi_j - \phi_i) \cdot \mathbf{r}_{ij}}{|\mathbf{r}_{ij}|^2} w(|\mathbf{r}_{ij}|) \quad (17)$$

$$\langle \nabla^2 \phi \rangle_i = \frac{2d}{\lambda n^0} \sum_{j \neq i} (\phi_j - \phi_i) w(|\mathbf{r}_{ij}|) \quad (18)$$

$$\lambda = \frac{\sum_{j \neq i} |\mathbf{r}_{ij}|^2 w(|\mathbf{r}_{ij}|)}{\sum_{j \neq i} w(|\mathbf{r}_{ij}|)} \quad (19)$$

Where, ϕ is a physical quantity of the field and d is space dimension.

4. SIMULATION FLOW

Fig. 1 shows the simulation flow with the proposed method.

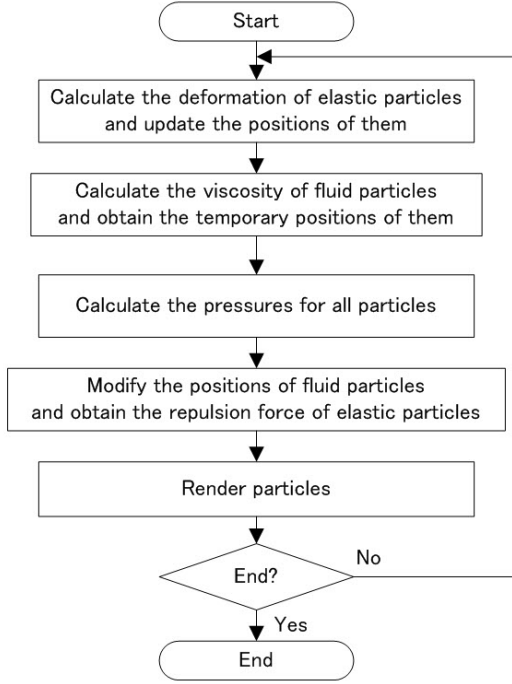


Fig.1: Simulation Flow.

4.1 Deformation of Elastic Body Particles

In case that the lame constant of elastic body is large, implicit dynamic calculation is needed to calculate the deformation of elastic body. First, the time derivative of Eq.(6) is discretized by taking second-order central difference as the following.

$$\frac{D^2 \mathbf{u}}{Dt^2} = \frac{\mathbf{u}^{t+1} - 2\mathbf{u}^t + \mathbf{u}^{t-1}}{\Delta t^2} \quad (20)$$

Next, the space derivative of Eq.(6) is discretized by applying MPS method as the following.

$$\langle \nabla(\nabla \cdot \mathbf{u}) \rangle_i = \frac{2d}{n^0} \sum_{j \neq i} \frac{\{(\mathbf{u}_j^{t+1} - \mathbf{u}_i^{t+1}) \cdot \mathbf{r}_{ij}^{t+1}\} \mathbf{r}_{ij}^{t+1}}{|\mathbf{r}_{ij}^0|^2 |\mathbf{r}_{ij}^{t+1}|^2} w(|\mathbf{r}_{ij}^0|) \quad (21)$$

$$\langle \nabla^2 \mathbf{u} \rangle_i = \frac{2d}{\lambda n^0} \sum_{j \neq i} (\mathbf{u}_j^{t+1} - \mathbf{u}_i^{t+1}) w(|\mathbf{r}_{ij}^0|) \quad (22)$$

Then, MPS method uses weight average. If multiple discretization such as that in Eq.(21) is necessary, weight average should be calculated only at the last discretization.

Finally, the simultaneous linear equation of displacement \mathbf{u}^{t+1} is obtained by substituting Eqs.(20)-(22) into Eq.(6).

$$\begin{aligned} & \rho_i \frac{u_i^{t+1} - 2u_i^t + u_i^{t-1}}{\Delta t^2} \\ &= (\lambda + G) \frac{2d}{n^0} \sum_{j \neq i} \frac{\{(\mathbf{u}_j^{t+1} - \mathbf{u}_i^{t+1}) \cdot \mathbf{r}_{ij}^{t+1}\} \mathbf{r}_{ij}^{t+1}}{|\mathbf{r}_{ij}^0|^2 |\mathbf{r}_{ij}^{t+1}|^2} w(|\mathbf{r}_{ij}^0|) \\ &+ \mu \frac{2d}{\lambda n^0} \sum_{j \neq i} (\mathbf{u}_j^{t+1} - \mathbf{u}_i^{t+1}) w(|\mathbf{r}_{ij}^0|) + \mathbf{F}_i \end{aligned} \quad (23)$$

BiCGSTAB (Biconjugate gradient stabilized) method is applied to solve the simultaneous linear equation. At this stage, not only displacement \mathbf{u}^{t+1} but also position \mathbf{r}^{t+1} are unknown. Therefore, the algorithm of Gauss-Seidel method is applied. It means that the displacement \mathbf{u}^{t+1} is calculated by approximating \mathbf{r}^{t+1} with \mathbf{u}^{t+1} in Eq.(23) at first. Then, the position \mathbf{r}^{t+1} is calculated from the displacement \mathbf{u}^{t+1} with Eq.(24). By substituting this value \mathbf{r}^{t+1} in Eq.(24) back into \mathbf{r}^{t+1} in Eq.(23) repeatedly, the accurate displacement \mathbf{u}^{t+1} can be obtained. The relationship between the displacement and the position of a particle is shown in Fig. 2.

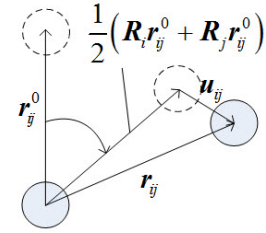


Fig.2: Relationship between Displacement and Position.

$$\mathbf{u}_j - \mathbf{u}_i = (\mathbf{r}_j - \mathbf{r}_i) - \frac{1}{2} (\mathbf{R}_i \mathbf{r}_{ij}^0 + \mathbf{R}_j \mathbf{r}_{ij}^0) \quad (24)$$

Where, \mathbf{R} is a rotation matrix which is determined from particle's orientation. Then, some particles of elastic body are attached to fixed rigid particles for satisfying the boundary condition in order to solve the simultaneous linear equation about \mathbf{r} in Eq.(24). The stress of elastic body is calculated by substituting displacement \mathbf{u} , which is obtained by Eq.(23), into Eq.(4) and by substituting Eq.(4) into Eq.(3).

4.2 Viscosity and Temporal Position of Fluid Particles

At first, the temporary velocity and the position due to external force, and the viscosity are calculated. In this calculation, the time step must be very small in explicit method since the blood viscosity becomes large when the velocity of blood stream becomes slow. Therefore, we use implicit method to obtain the stable result. The time derivative of Eq.(11) is discretized by taking forward difference as the following.

$$\frac{D\mathbf{v}}{Dt} = \frac{\mathbf{v}^{t+1} - \mathbf{v}^t}{\Delta t} \quad (25)$$

The space derivative of Eq.(11) is discretized with MPS method as follows.

$$\langle \nabla^2 \mathbf{v} \rangle_i = \frac{2d}{\lambda n^0} \sum_{j \neq i} (\mathbf{v}_j^{t+1} - \mathbf{v}_i^{t+1}) w(|\mathbf{r}_{ij}^{t+1}|) \quad (26)$$

The simultaneous linear equation of velocity \mathbf{v}^{t+1} is derived by substituting Eqs.(25) and (26) into Eq.(11) except for the pressure term as shown in Eq.(27).

$$\rho_i = \frac{\mathbf{v}_j^{t+1} - \mathbf{v}_i^t}{\Delta t} = \mu \frac{2d}{\lambda n^0} \sum_{j \neq i} (\mathbf{v}_j^{t+1} - \mathbf{v}_i^{t+1}) w(|\mathbf{r}_{ij}^{t+1}|) + \mathbf{F}_i \quad (27)$$

Note that the external force in Eq.(27) is limited to the gravity because the repulsive force between particles can be calculated from the pressure calculation, which is described later. Since the particle position \mathbf{r}^{t+1} is not also known, the algorithm of Gauss-Seidel method is applied as well as the deformation calculation of the elastic body.

4.3 Pressure and Repulsive Force

In this method, in order to calculate the repulsive force between the fluid and the elastic body, the temporary pressure of the elastic body is needed. In the previous method, particles with low particle density are defined as free surface particles and their pressure are fixed to zero. The repulsive force between free surface particles is always zero since the gradient of the pressure of free surface particles becomes zero. Therefore, our method treats particles inside free surface and ones on it equally to calculate the repulsive force by using virtual particles.

At First, since the physical density is proportional to the particle density Eq. (2) can be rewritten with Eq.(28).

$$\frac{Dn}{Dt} + n^0 \nabla \cdot \mathbf{v} = 0 \quad (28)$$

The pressure term of Eq.(11) can be expressed as (29) by excluding the viscosity term and the external force.

$$\rho \frac{D\mathbf{v}}{Dt} = -\nabla p \quad (29)$$

By solving Eq.(29) for \mathbf{v} and by substituting \mathbf{v} into Eq.(28), Poisson equation of pressure can be obtained as follows.

$$\nabla^2 p = -\frac{\rho}{n^0 \Delta t} \frac{n^* - n^0}{\Delta t} \quad (30)$$

Where, n^* is the particle density at the temporal position. By discretizing Eq.(30) with MPS method, the following simultaneous linear equation about p can be obtained. The repulsive calculation is also performed at the same time by treating the elastic body particle and the fluid particle identically.

$$\frac{2d}{\lambda n^0} \sum_{j \neq i} (p_j - p_i) w(|\mathbf{r}_{ij}^*|) = \frac{\rho}{n^0 \Delta t} \frac{n^* - n^0}{\Delta t} \quad (31)$$

Eq.(31) can be expressed with a matrix as follows.

$$\frac{2d}{\lambda n^0} \begin{bmatrix} -n_i^* & \cdots & w(|\mathbf{r}_{ij}^*|) \\ \vdots & \ddots & \vdots \\ w(|\mathbf{r}_{ij}^*|) & \cdots & -n_j^* \end{bmatrix} \begin{bmatrix} p_i \\ \vdots \\ p_j \end{bmatrix} = \begin{bmatrix} -\frac{\rho}{n^0 \Delta t} \frac{n_i^* - n^0}{\Delta t} \\ \vdots \\ -\frac{\rho}{n^0 \Delta t} \frac{n_j^* - n^0}{\Delta t} \end{bmatrix} \quad (32)$$

The boundary condition is necessary to solve Eq.(32) since the coefficient matrix is not strict diagonal dominant. As the boundary condition, the pressure of free surface particles with low particle density is considered as zero. Then, no repulsive force is generated on free surface.

To overcome this problem, particles on free surface and ones inside of it should be treated with the same way by assuming the existence of uncompressed virtual particles with zero pressure in the space, where no particle is found. The image of virtual particles is shown in Fig. 3. The virtual particles are assumed to exist in the shaded region of Fig. 3.

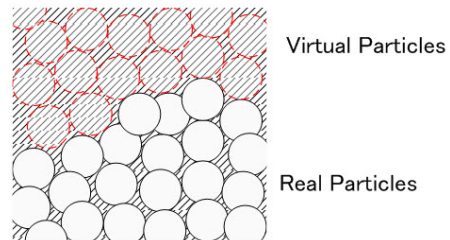


Fig.3: Virtual and Real Particles.

For example, when virtual particles m exist, Eq.(32) becomes Eq.(33) and the pressure of particles on free surface can be calculated.

$$\begin{aligned}
& \frac{2d}{\lambda n^0} \begin{bmatrix} -n_i^{**} & \cdots & w(|\mathbf{r}_{ij}^*|) & \cdots & w(|\mathbf{r}_{im}^*|) \\ \vdots & \ddots & \vdots & \ddots & \vdots \\ w(|\mathbf{r}_{ji}^*|) & \cdots & -n_j^{**} & \cdots & w(|\mathbf{r}_{jm}^*|) \\ \vdots & \ddots & \vdots & \ddots & \vdots \\ 0 & \cdots & 0 & \cdots & 1 \end{bmatrix} \begin{bmatrix} p_i \\ \vdots \\ p_j \\ \vdots \\ p_m \end{bmatrix} \\
&= \begin{bmatrix} -\frac{\rho}{n^0 \Delta t} \frac{n_i^{**} - n^0}{\Delta t} \\ \vdots \\ -\frac{\rho}{n^0 \Delta t} \frac{n_j^{**} - n^0}{\Delta t} \\ \vdots \\ 0 \end{bmatrix}
\end{aligned} \quad (33)$$

Where, n^{**} is the density of particles at the space where virtual particles are placed. Here, Eq.(33) becomes Eq.(34) because the pressure of virtual particles is zero.

$$\frac{2d}{\lambda n^0} \begin{bmatrix} -n_i^{**} & \cdots & w(|\mathbf{r}_{ij}^*|) \\ \vdots & \ddots & \vdots \\ w(|\mathbf{r}_{ji}^*|) & \cdots & -n_j^{**} \end{bmatrix} \begin{bmatrix} p_i \\ \vdots \\ p_j \end{bmatrix} = \begin{bmatrix} -\frac{\rho}{n^0 \Delta t} \frac{n_i^{**} - n^0}{\Delta t} \\ \vdots \\ -\frac{\rho}{n^0 \Delta t} \frac{n_j^{**} - n^0}{\Delta t} \end{bmatrix} \quad (34)$$

For the purpose of explanation, we have placed virtual particles; however the virtual particles does not exist on the simulation because the virtual particle is a conceptual particle. For the reason, the particle density with virtual particles, n^{**} , cannot be calculated by summation with the weight function w . Therefore, the particle density with virtual particles, n^{**} , can be calculated with the particle density increased by adding overlapping particles to the initial uncompressed state n^0 . Volume ratio, which is the ratio of overlapped particles over all ones, is calculated with Eq.(35). Fig. 4 shows the overlapped state by two particles.

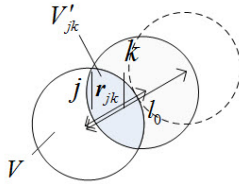


Fig.4: Overlap between Particles.

$$\alpha'_{jk} = \frac{V'_{jk}}{V} = \frac{l_0 - |\mathbf{r}_{jk}|}{l_0} \quad (35)$$

Where, α' is volume ratio, V is a particle volume, V' is the overlapped volume, and l_0 is the distance between particles in uncompressed state. The summation of the volume ratio becomes the total space overlapped by particles.

$$\alpha_j = \sum_{j \neq m} \alpha'_{jm} \quad (36)$$

The particle density with virtual particles is calculated with Eq.(37) if the number of particles increases according to the overlapped space. The volume ratio becomes the half because the two particles have the same common space to each other. Fig. 5 shows the improvement of the particle density.

$$n_i^{**} = n_0 + \frac{1}{2} \sum_{j \neq i} w(|\mathbf{r}_{ij}|) \alpha_j \quad (37)$$

For stable calculation, the particle density with virtual particles, n^{**} , is replaced with the particle density n^* when n^{**} is smaller than n^* . The pressure is calculated with the above particle density n^{**} .

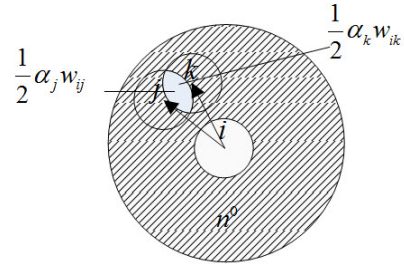


Fig.5: Improvement of the Particle Density.

Finally, after the gradient of pressure is calculated, the repulsive force among the elastic bodies and the repulsive force between the fluid and the elastic body are calculated. In this step, the gradient of pressures of the elastic body particles is not calculated with the particles, which are placed at the initial positions, because the repulsive force is already calculated with the governing equation of the elastic body. Then, we consider the force received by the elastic body particles as the external force in the deformation calculation, and use it in the next step. In order to take the pressure of virtual particles into account, the pressure of a virtual particle that is placed at the symmetric position of a real particle, is considered as zero and then the pressure is calculated with Eq.(38). (See Fig.6)

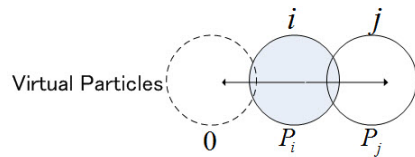


Fig.6: Virtual Particle Placed at the Symmetry Position.

$$\begin{aligned}\nabla p &= \frac{d}{n^0} \sum_{j \neq i} \frac{(0 - p_i)(-\mathbf{r}_{ij})}{|\mathbf{r}_{ij}|^2} + \frac{(p_j - p_i)\mathbf{r}_{ij}}{|\mathbf{r}_{ij}|^2} w(|\mathbf{r}_{ij}|) \\ &= \frac{d}{n^0} \sum_{j \neq i} \frac{p_j \mathbf{r}_{ij}}{|\mathbf{r}_{ij}|^2} w(|\mathbf{r}_{ij}|)\end{aligned}\quad (38)$$

5. RESULT

The simulations of opening and closing of the aortic valve and blood stream inside of the aorta, have been performed.

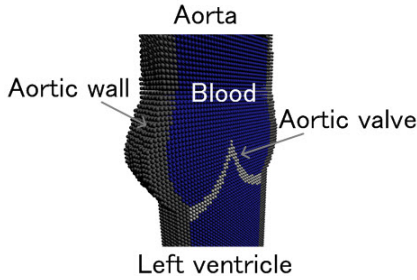


Fig. 7: Simulation Model of the Aorta.

Fig. 7 shows the image of the simulation model that is cut at a cross section. The particles composing of the aorta wall, blood and the aortic valve are about 60k fixed rigid particles, about 64k fluid particles and 3k elastic body particles, respectively. The aortic valve has the parameters of 1M[Pa] Young's modulus and 0.49 Poisson's ratio.

Fig. 8 shows the result of the simulation. The left and right figures show the pressure distribution of the blood and the stress distribution of the aortic valve, respectively. In the initial state (Fig. 8(a)), the pressure and the stress of all particles are 0[Pa], and the blood flows at the velocity of 1.0[m/s] from the left ventricle side to the aorta. As the blood flows, the internal pressure of the left ventricle increases to 20k[Pa], and the blood flows to the aorta when the aortic valve opens (Fig. 8(b)). The stress at the bottom of the aortic valve is larger than that at the tip of the value. When the left ventricular pressure becomes 0[Pa], the aortic valve is closed since the pressure caused by the blood stream becomes small (Fig. 8(c)). When the blood flows backward from the aorta to the left ventricle, the internal pressure of the aortic valve becomes larger than that of the left ventricle, and the aortic valve closes (Fig. 8(d)).

6. CONCLUSION

We have performed the 3D simulation of the aorta with a particle method, which visualizes the blood stream and the stress distribution on the aortic valve for the surgeries of the aortic valve replacement and/or the aortic valve plasty. In our simulation, the

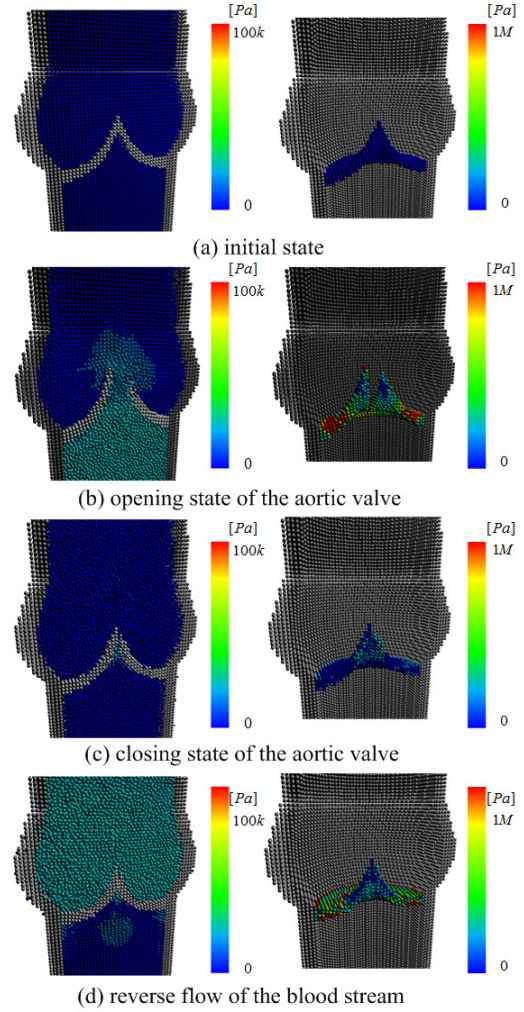


Fig. 8: Visualization of the Pressure and the Stress Distribution.

aortic valve is treated as the elastic body and the blood is treated as Herschel-Bulkley fluid. The deformation has been calculated by an implicit method using MPS in order to perform stable transformation. In addition, the pressure of the fluid and the repulsive force between surface particles of the fluid can be calculated by considering virtual particles. Furthermore, we have been able to obtain the repulsive force between blood and the aortic valve, and also the force between the aortic valves by considering all particles for the pressure calculation.

This method has made it possible to simulate the aortic valve movement and to visualize the pressure and the stress according to it. The aortic model has been built based on the image data of a real patient and the movement has been evaluated by comparing the simulation result with a real US (Ultrasound) echo movie. From the clinical point of view, the aortic valve movement and the value of the pressure and the stress are similar to the real one, however, the opening and the closing of the valve is a little bit smooth while the real movement of it is more dynamic and

the valve opens more widely. Therefore, we have to consider the movement by the muscle of the aortic valve and also plan to perform the simulation with the medical data of a real patient.

7. ACKNOWLEDGMENT

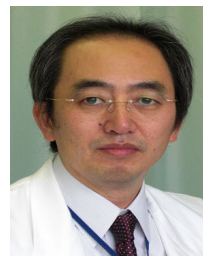
This research was supported by Japan Society for the Promotion of Science (Research No.21500125).

References

- [1] Tatsuta Arai, *Surgery of the cardiac valvulopathy*, Igaku-shoin, 2003.
- [2] S. Koshizuka, *Particle Method*, Maruzen, 2005.
- [3] A. Khayyer, H. Gotoh and S. Shao, "Corrected incompressible SPH method for accurate water surface tracking in breaking waves," *Coastal Engineering*, vol.55, no.3, pp.236–250, 2008.
- [4] M. Tanaka and S. Koshizuka, "Simulation of Red Blood Cell Deformation Using a Particle Method," *Journal of Japan Society of Fluid Mechanics*, vol.26, no.1, pp.49–55, 2007.
- [5] M. Nakagawa, N. Mukai, K. Niki and S. Takanashi, "A Bloodstream Simulation Based on Particle Method," *Medicine Meets Virtual Reality 18*, IOS Press, pp.389–393, 2011.
- [6] K. M. Prasad and G. Radhakrishnamacharya, "Flow of Herschel-Bulkley fluid through an inclined tube of non-uniform cross-section with multiple stenoses," *Archives of Mechanics*, vol.60, no.2, pp.161–172, 2008.



Kiyomi Niki received her B.E. from Saga Medical University and entered Tokyo Women's Medical University in 1985. She became an assistant professor in 1993 and received M.D. in 1994, respectively. She then became a lecturer and an associate professor in 2004 and 2005, respectively. She also became a visiting professor and a professor at Waseda University and Musashi Institute of Technology in 2006 and 2007, respectively. She is now a professor at Tokyo City University. Her current research interest is diagnoses with ultrasonic waves in circulatory organs.



Shuichiro Takanashi received his B.E. in school of medicine from Ehime University in 1984. He became a chief of surgery department at New Tokyo Hospital and Sakakibara Heart Institute in 2001 and 2004, respectively. He is now a medical instructor of the Japanese Association for Thoracic Surgery, a mediator of AHVS/OPCAB, a director of Japanese Association for Coronary Artery Surgery, a councilor of the Japanese Society for Cardiovascular Surgery, a director of the Japanese Coronary Association and a member of the Society of Thoracic surgeons. He now performs about 400 heart surgeries a year.



Masashi Nakagawa received his B.E. and M.E. degrees in computer and media engineering and electrical engineering from Musashi Institute of Technology in 2007 and 2009, respectively and also received Ph.D. degree in information engineering from Tokyo City University in 2012. He entered Canon Inc. in 2012. He was researching medical application systems by using computer graphics.



Nobuhiko Mukai received his B.E. and M.E. degrees in mechanical engineering from Osaka University in 1983 and 1985, respectively. He joined Mitsubishi Electric Corp. in 1985. He also entered Cornell University in 1995 and received his M.E. degree in computer science in 1997. In 2000, he entered Osaka University and received his Ph.D. degree in systems and human science in 2001. He then joined Musashi Institute

of Technology as an associate professor in 2002 and has become a professor in 2007. He is now a professor at Tokyo City University. His current research interests are computer graphics, image processing, virtual reality and medical applications.